Journal of Applied Mechanics and Technical Physics, Vol. 42, No. 2, pp. 284–289, 2001

MULTI-FRONT PHASE TRANSITIONS DURING NONISOTHERMAL FILTRATION OF LIVE PARAFFIN-BASE CRUDE

R. F. Sharafutdinov

UDC 532.546

By numerical modeling of nonisothermal filtration of multicomponent oil with allowance for the Joule–Thomson effect, adiabatic effect, and heat of phase transitions that occur during oil degassing and paraffin crystallization, the formation of profiles of phase-saturation, concentrations of oil components, and temperature in oil beds is studied. It is shown that consideration of many components results in occurrence of phase-transition fronts during degassing of oil components and paraffin crystallization. In turn, paraffin crystallization gives rise to temperature oscillations. Depending on the initial paraffin concentration and on the ratio of phase-transition heats for oil degassing and paraffin crystallization in an oil bed, either decaying or steady-state temperature oscillations are observed.

As is well known, oil is a mixture of various hydrocarbons, which, under actual bedded conditions, occur in gaseous, liquid or solid states. Conventionally, oil may be considered as a three-component system composed of a light (C_1–C_3), a medium (C_4–C_6), and a heavy (more complex than C_6) components. The solid components of oil include paraffin [1].

The temperature distribution in an oil bed during nonisothermal filtration is caused by the Joule–Thomson and adiabatic effects, and, additionally (for pressures above the saturation pressure), by the heat of liquid degassing [2]. On attaining a pressure in the bed below the pressure of oil saturation with gas, oil degassing occurs, and the temperature decreases [2]. Simultaneously, the temperature in the oil bed may be lower than the paraffin-crystallization point, which results in paraffin precipitation accompanied by heat release [1]. Thus, oil degassing and paraffin crystallization result in a temperature decrease and increase, respectively. The thermal probing of oil wells and beds is based on regularities of temperature variations [3].

Available mathematical models of the temperature field with allowance for the Joule–Thomson effect, adiabatic effect, and oil-degassing heat were developed for filtration of live crude and water without allowance for the multitude of oil components and paraffin crystallization [2].

In the present paper, the temperature field in an oil bed, formed during filtration of a three-component oil, is numerically studied with allowance for oil degassing and paraffin crystallization. The diffusional transport of oil components, transport of liquid and gaseous phases caused by the capillary pressure jump in the phases, and longitudinal heat transfer due to heat conduction are ignored.

Heat losses being neglected, we formulate a mathematical model for calculating temperature distributions caused by the Joule–Thomson effect, adiabatic effect, and phase-transition heat during degassing of the light and medium components of oil with due allowance made for paraffin crystallization during filtration of live crude in an oil bed. In the first approximation, we may distinguish four phases [porous "sponge" (0), gas phase (1), oil (2), and paraffin (3)] and three components that take part in heat- and mass-transfer processes [light component (1), medium component (2), and heavy component (paraffin) (3)].

Bashkir State University, Ufa 450000. Translated from Prikladnaya Mekhanika i Tekhnicheskaya Fizika, Vol. 42, No. 2, pp. 111–117, March–April, 2001. Original article submitted November 20, 1998; revision submitted September 18, 2000.

 0021-8944/01/4202-0284 $25.00

The equations of mass conservation of the phases and components, the equation of motion in the form of the Darcy law, and the equation of heat inflow for a plane radial case have the following form:

$$\frac{\partial(m\rho_i S_i)}{\partial t} + \frac{1}{r}\frac{\partial(rm\rho_i S_i V_i)}{\partial r} = I_{ij}, \quad I_{ii} = 0 \quad (i \neq j); \tag{1}$$

$$\frac{\partial(m\rho_i C_{ik} S_i)}{\partial t} + \frac{1}{r}\frac{\partial(rm\rho_i S_i C_{ik} V_i)}{\partial r} = -I_{ijk}, \quad I_{iik} = 0 \quad (i \neq j, \quad i = 1,\, 2, \quad k = 1,\, 2,\, 3); \tag{2}$$

$$\frac{\partial(m\rho_3 S_3)}{\partial t} = I_{23}; \tag{3}$$

$$mS_i V_i = -\frac{Kk_i}{\mu_i}\frac{\partial P}{\partial r} \qquad (i = 1,\, 2); \tag{4}$$

$$\frac{\partial}{\partial t}\left[(1-m)\rho_0 c_0 T + \sum_{i=1}^{3} m\rho_i c_i S_i T + m\rho_1 S_1 C_{11} L_{11} + m\rho_1 S_1 C_{12} L_{12} + m\rho_3 S_3 L_3\right]$$

$$+ \frac{1}{r}\frac{\partial}{\partial r}\left[r\left(m\sum_{i=1}^{2}\rho_i c_i S_i V_i T + m\rho_1 S_1 V_1 C_{11} L_{11} + m\rho_1 S_1 V_1 C_{12} L_{12}\right)\right]$$

$$+ m\sum_{i=1}^{2}\rho_i c_i S_i V_i \varepsilon_i \frac{\partial P}{\partial r} - m\sum_{i=1}^{3}\rho_i c_i S_i \eta_i \frac{\partial P}{\partial t} = 0; \tag{5}$$

$$\sum_{i=1}^{3} S_i = 1, \qquad \sum_{k=1}^{2} C_{1k} = 1, \qquad \sum_{k=1}^{3} C_{2k} = 1. \tag{6}$$

Here the subscripts i, j, and k refer to different phases and components of the mixture, S_i and V_i are the saturation and velocity of the ith phase, C_{ik} is the concentration of the kth component in the ith phase, ρ_i is the density of the ith phase, K is the absolute permeability, k_i is the phase permeability, μ_i is the viscosity of the ith phase, m is the porosity, P is the pressure, T is the temperature, c_i is the heat capacity, ε_i is the Joule–Thomson coefficient, η_i is the adiabatic coefficient, L_{11} is the heat of degassing of the first (light) component, L_{12} is the heat of degassing of the second (medium) component, and L_3 is the paraffin-crystallization heat.

The initial and boundary conditions are

$$\begin{aligned}
&t = 0, \quad r > 0: && S_i = S_{i0}, \quad C_{ik} = C^0_{ik}, \quad P = P_0, \quad T = T_0,\\
&t > 0, \quad r = R_0: && P = P_{\mathrm{b}}(t), \quad P^0_{\mathrm{b}} \leqslant P_{\mathrm{b}}(t) \leqslant P_0,\\
&t > 0, \quad r = R: && P = P_0, \quad S_i = S^0_i, \quad T = T_0.
\end{aligned} \tag{7}$$

Here R_0 and R are the radius of the oil well and that of the external boundary of the reservoir.

The closing relations for Eqs. (1)–(7) depend on the phase state of the three-component system. For $P > P_{1\mathrm{s}}$, $P > P_{2\mathrm{s}}$, and $T > T_{\mathrm{cr}}$, the system is in a single-phase state ($P_{1\mathrm{s}}$ and $P_{2\mathrm{s}}$ are the saturations pressure of oil with the first and second components, respectively, and T_{cr} is the paraffin crystallization temperature). In the case of interest, we have $S_1 = 0$, $S_3 = 0$, $I_{12\,1} = I_{12\,2} = I_{23} = 0$, $C_{21} = C^0_{21}(T_0, P_0)$, and $C_{22} = C^0_{22}(T_0, P_0)$. For $P \leqslant P_{1\mathrm{s}}$, $P > P_{2\mathrm{s}}$, and $T > T_{\mathrm{cr}}$, the system is in a two-phase state ($S_1 \neq 0$, $S_2 \neq 0$, and $S_3 = 0$), and the concentration of the first component is temperature- and pressure-dependent, i.e., $C_{21} = C_{21}(T, P)$. For $P \leqslant P_{1\mathrm{s}}$, $P \leqslant P_{2\mathrm{s}}$, and $T > T_{\mathrm{cr}}$, the system is also in a two-phase state ($S_1 \neq 0$, $S_2 \neq 0$, and $S_3 = 0$); in this case, we have $C_{21} = C_{21}(T, P, C_{11})$ and $C_{22} = C_{22}(T, P, C_{12})$. In a three-phase state ($P \leqslant P_{1\mathrm{s}}$ and $T \leqslant T_{\mathrm{cr}}$), the concentrations of the gas (first component) and paraffin contained in oil (without allowance for degassing of the second component) are related by relations $C_{21} = C_{21}(T, P)$ and $C_{23} = C_{23}(T, P)$.

The solubility of pure gases was assumed to obey the Henry law. The mass concentrations were calculated by the formula $C_{i1} = (1 + \alpha P/(\rho_1 \beta))^{-1}$ using the values of the Henry coefficients α for the bed-mean temperature and the volume expansion coefficient of oil β reported in [4]. For the gas mixture, the Raoult

law was used. The relative phase permeabilities were used as reported in [5]. The oil and gas densities are functions of pressure, temperature, and concentrations of components [4]. To calculate the gas-phase density, the formula $P = \rho_1 RT \sum_{k=1}^{2} C_{ik}/M_k$ was used, where R is the universal gas constant and M_k is the molecular weight of the kth component. The density of the oil phase is given by the formula $\rho_2 = \Big(\sum_{k=1}^{3} C_{2k}/\rho_k^0\Big)^{-1}$, where ρ_k^0 is the density of the kth component for $P = P_0$ and $T = T_0$. The absolute permeability depends on the saturation of the oil bed with paraffin and is given by the Kozeny formula [4] $K = K_0 m'^3/(1-m')^2$, where K_0 is the absolute permeability and $m' = m(1 - S_3)$. The oil viscosity is a function of component concentrations and is given by the formula [6] $\ln \mu_2 = \sum_{k=1}^{3} C_{2k} \ln \mu_{2k}$, where μ_{2k} is the viscosity of the kth component for $P = P_0$ and $T = T_0$. The thermophysical parameters of the phases c_i, ε_i, η_i, L_{11}, L_{12}, and L_3 were assumed constant; their numerical values were taken from tables for the bed-mean pressure $P = P_0$ and temperature $T = T_0$.

The equation for pressure may be obtained by substituting (4) into Eqs. (1)–(3) with subsequent summation of resultant relations over components and phases:

$$\frac{\partial}{\partial t}\Big(m \sum_{i=1}^{3} \rho_i S_i\Big) - \frac{1}{r}\frac{\partial}{\partial r}\Big(rK \sum_{i=1}^{2} \frac{k_i \rho_i}{\mu_i}\frac{\partial P}{\partial r}\Big) = 0.$$

This equation may be also rewritten as

$$\frac{1}{r}\frac{\partial}{\partial r}\Big(B\frac{\partial P}{\partial r}\Big) = \frac{\partial F}{\partial t}, \tag{8}$$

where $B = rK \sum_{i=1}^{2} \frac{k_i \rho_i}{\mu_i}$ and $F = m \sum_{i=1}^{3} \rho_i S_i$.

The equations for the oil and paraffin saturation are found from Eq. (2) by summation over components; they have the form

$$\frac{\partial (m\rho_2 C_{22} S_2)}{\partial t} - \frac{1}{r}\frac{\partial}{\partial r}\Big(rKk_2 \frac{C_{22}\rho_2}{\mu_2}\frac{\partial P}{\partial r}\Big) = 0; \tag{9}$$

$$\frac{\partial [m(\rho_2 C_{23} S_2 + \rho_3 S_3)]}{\partial t} - \frac{1}{r}\frac{\partial}{\partial r}\Big(rKk_2 \frac{C_{23}\rho_2}{\mu_2}\frac{\partial P}{\partial r}\Big) = 0. \tag{10}$$

System (8), (9) was solved numerically using a conservative finite-difference count-through scheme. The saturation of the phases and the temperature were calculated using an explicit scheme, whereas the pressure was calculated by an implicit scheme. A sweep equation for pressure emerges after some rearrangement of Eq. (8):

$$\alpha_n P_{n-1} - c_n P_n + b_n P_{n+1} = -f_n, \qquad \alpha_n = \sum_{i=1}^{3} B_{i-1}^j \tau, \quad b_n = \sum_{i=1}^{3} B_i^j \tau,$$

$$c_n = \sum_{i=1}^{3} (B_i^j + B_{i-1}^j)\tau, \qquad f_n = r_n \chi^2 \sum_{i=1}^{3} (m\rho_i^j S_i^{j+1} - m\rho_i^j S_i^j).$$

Here χ in the step over the coordinate. First, the saturation of the phases and the pressure are to be found, and then the temperature distribution can be calculated. The calculation scheme may be represented as follows:

$$\frac{\Phi_n^{j+1} - \Phi_n^j}{\tau} - \frac{B_n^j (P_{n+1}^j - P_n^j) - B_{n-1}^j (P_n^j - P_{n-1}^j)}{r_n \chi^2} = 0.$$

Here Φ_n^j is the mass of a component or a phase or the specific heat content in the nth cell on the jth time layer and τ is the time step.

With the Courant conditions fulfilled for the most rapidly traveling front, the scheme described above is monotonic and stable. The stability condition for multiphase, multicomponent filtration cannot be obtained

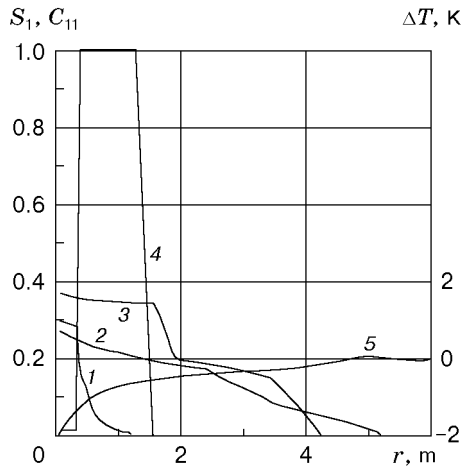

Fig. 1

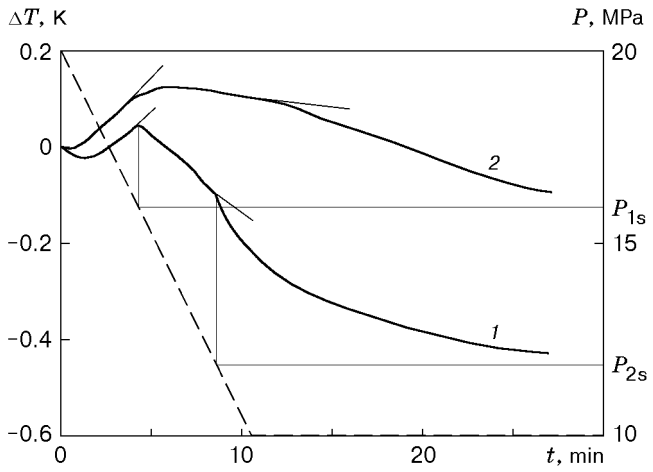

Fig. 2

Fig. 1. Distributions of the gas-phase saturation S_1 (curves 1–3), concentration of the first component C_{11} (curve 4), and temperature T (curve 5) along the oil bed after the beginning of filtration for $t = 5$ (1 and 4), 20 (2), and 60 min (3).

Fig. 2. Time dependences of the temperature (solid curves) and pressure (dashed curve) at the oil-bed outlet: curves 1 is the predicted dependence and curve 2 refers to the data for oil well No. 2610 of the Talinsk oil pool.

analytically; therefore, the stability was checked experimentally in the course of calculations by varying the time step. For problems of this kind, with the spatial step $\chi = 0.1$ m, the time step τ should be smaller than 0.05 sec. For $\tau > 0.05$ sec, the calculations become unstable. The solution has the first order of accuracy with respect to time and the second order with respect to the coordinate. The test on convergence shows that, as the time step τ decreases from 0.04 to 0.001 sec, the magnitude of the sought functions changes only in the third decimal digit. The numerical error does not exceed 5% for the time step $\tau = 0.04$ sec, and for time steps smaller than $\tau = 0.001$ sec, the magnitude of the functions of interest remains almost unchanged.

The numerical solution of the above-formulated problem was validated by comparing the predicted time dependence of the temperature at the oil-bed outlet with the known analytical solution for the temperature field caused by the barothermal effect (variation of the liquid temperature caused by the Joule–Thomson effect and by the adiabatic effect in a nonstationary pressure field) during filtration of single-phase, single-component oil [3], and also by comparing the numerical results with the data for oil well No. 2610 of the Talinsk oil pool (Russia, Western Siberia).

Predicted temperature fields and saturation of the phases during oil filtration, which were obtained with due allowance for degassing of the light and medium oil components, and also those obtained during filtration of live crude with paraffin crystallization after oil-well start-up are presented below.

In calculating the temperature field, the numerical values of thermodynamic parameters of the phases, in line with actual oil-bed data, varied within the following ranges [4]: $c_1 = 2000$–4000 J/(kg · K), $c_2 = c_3 = 1600$–2400 J/(kg · K), $\varepsilon_1 = (-2)$–(-4) K/MPa, $\varepsilon_2 = 0.16$–0.56 K/MPa, initial mass concentration of paraffin in oil $C_{23}^0 = 0.001$–0.050, initial oil-bed pressure $P_0 = 16$–20 MPa, and minimum pressure at the oil-bed boundary ($r = R_0$) $P_{\rm b}^0 = 9$–14 MPa.

The calculation results are shown in Figs. 1–5 ($\Delta T = T - T_0$). The following values of thermodynamic parameters of the phases were used: $c_0 = 800$ J/(kg · K), $c_1 = 3000$ J/(kg · K), $c_2 = c_3 = 2000$ J/(kg · K), $\varepsilon_1 = -4$ K/MPa, $\varepsilon_2 = 0.4$ K/MPa, $\eta_1 = 20$ K/MPa, and $\eta_2 = \eta_3 = 0.13$ K/MPa. The phase-transition heat during oil degassing was estimated using the data reported in [7, 8]; it varied within the following ranges: $L_{11} = 50$–300 kJ/kg, $L_{12} = 100$–400 kJ/kg, and paraffin crystallization heat was $L_3 = 200$–500 kJ/kg [2]. The viscosities of the gas phase and the oil-phase components were assumed to be identical: $\mu_1 = 0.01$ mPa · sec, $\mu_{21} = 0.1$ mPa · sec, $\mu_{22} = 0.4$ mPa · sec, and $\mu_{23} = 4$ mPa · sec. The oil-bed pressure was $P_0 = 20$ MPa, the pressure at the bed (well) boundary was $P_{\rm b}^0 = 10$ MPa, and the oil saturation pressure with gas was $P_{1\rm s} = 18$ MPa and $P_{2\rm s} = 16$ MPa.

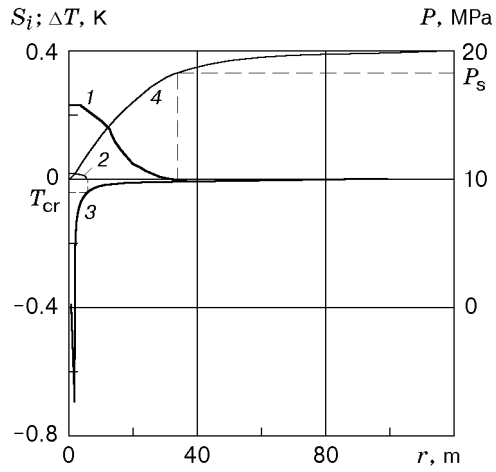

Fig. 3

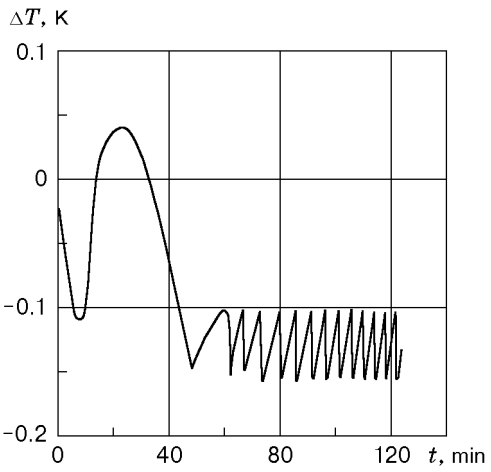

Fig. 4

Fig. 3. Distributions of the saturations for the gas (1) and paraffin (2), temperature (3), and pressure (4) along the oil bed for $t = 60$ min.

Fig. 4. Time dependence of the temperature at the oil-bed outlet for $C_{23}^0 = 0.05$ and $L_3/L_1 = 2$–5.

Figure 1 shows the distributions of temperature, gas saturation and concentration of the first component along the oil bed after the moment at which the pressure at the oil-bed outlet starts decreasing (after the well start-up). This figure shows two phase-transition fronts that correspond to oil degassing at $P \leqslant P_{1s}$ and $P \leqslant P_{2s}$. In the phase-transition fronts, there are jumps (abrupt changes) of phase saturation and concentrations of the components. The first jump of saturation is formed in the phase-transition front of the first component at $P = P_{1s}$, and the second at $P = P_{2s}$. A slight increase in temperature in a remote region where no oil degassing occurs (gas-phase saturation equals zero) and a temperature decrease in the oil-degassing region are observed. Simultaneously, a change in the temperature gradient is observed in the phase-transition fronts of the first and second components of oil.

Figure 2 shows the time dependences of temperature and pressure after the oil-well start-up with allowance for degassing of multicomponent oil. The curves exhibit sections with differential degassing of oil components, which are characterized by some change in the temperature gradient (degassing of the first and second components occurs at $P = 16$ and 11 MPa, respectively).

The effect of oil degassing and paraffin crystallization on the temperature field is illustrated by Figs. 3–5. Figure 3 shows the distributions of the gas and paraffin saturation, temperature and pressure along the oil bed. One can see two phase-transition fronts caused by oil degassing at $P < P_{1s}$ and paraffin crystallization at $T < T_{cr}$. In the phase-transition front that corresponds to the pressure isobar of oil saturation with gas, there is a jump of the gas saturation (curve 1). Oil degassing results in a decrease in the fluid temperature in the bed (curve 3). In the phase-transition front that corresponds to the flow temperature below the paraffin-crystallization point, there is a jump of the paraffin saturation.

It follows from the calculation results that, for the chosen values of ε_i and η_i, and also for the chosen bottom-hole and oil-bed pressures, the formation of the temperature field in the oil bed depends on the initial concentration of paraffin in oil and also on the ratio of phase-transition heats during oil degassing and paraffin crystallization.

Figure 4 shows the time dependence of the bed-outlet temperature for $C_{23}^0 = 0.05$ and $L_3/L_1 = 2$–5. On attaining a pressure below the pressure of oil saturation with gas, oil degassing and gas accumulation start, and the temperature decreases owing to the action of the degassing heat and adiabatic expansion and throttling of the gas. On attaining a flow temperature below the paraffin-crystallization point, oil gives off paraffin. During paraffin crystallization and heat release, the temperature-decrease rate diminishes and, beginning from a certain moment, the temperature start increasing. For a temperature above the paraffin-

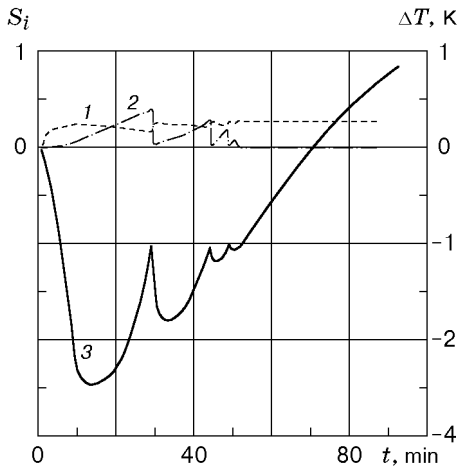

Fig. 5. Saturations for the gas (1) and paraffin (2) and temperature (3) at the oil-bed outlet versus time ($C_{23}^0 = 0.01$ and $L_3/L_1 = 1$).

crystallization point, paraffin completely dissolves in oil, and filtration of live crude is observed in the flow. An abrupt decrease in the temperature dependence corresponds to this moment. As the temperature further decreases, the processes of formation of gas and paraffin saturation are reproduced again.

Thus, for the chosen ratios between the phase-transition heat and initial concentration of paraffin, the effects caused by oil degassing and paraffin crystallization give rise to temperature oscillations in the oil bed.

Figure 5 illustrates the decay of temperature oscillations for $C_{23}^0 = 0.01$ and $L_3/L_1 = 1$. In this case, after the temperature drop owing to oil degassing and the temperature rise caused by paraffin crystallization and liquid-phase throttling, the temperature oscillation decay, and a monotonic increase in temperature is observed. It is also seen from Fig. 5 that the periods of temperature increase and decrease correlate with variations in gas and oil saturation. Finally, the oil heating due to throttling prevails over its cooling during degassing.

The results obtained in this study supplement available data on the formation of temperature distributions under actual oil-bed conditions as the pressure decreases to values below the pressure of oil saturation with gas. These data can be used in interpreting the results of temperature probing of oil wells during oil degassing.

REFERENCES

1. S. F. Lyushin, V. A. Rasskazov, D. M. Sheikh-Ali, et al., *Prevention of Paraffin Precipitation in Oil Production* [in Russian], Gostoptekhizdat, Moscow (1961).
2. R. A. Valiullin, A. Sh. Ramazanov, and R. F. Sharafutdinov "Barothermal effect during three-phase filtration with phase transitions," *Izv. Ross. Akad. Nauk, Mekh. Zhidk. Gaza*, No. 6, 113–117 (1994).
3. R. A. Valiullin and A. Sh. Ramazanov, *Thermal Probing during Compressor Development of Wells* [in Russian], Izd. Bashkir. Univ., Ufa (1992).
4. Sh. K. Gimatudinov and A. I. Shirkovsky, *Physics of Oil and Gas Beds* [in Russian], Nedra, Moscow (1982).
5. K. M. Fedorov and R. F. Sharafutdinov, "Theory of nonisothermal filtration with phase transitions," *Izv. Akad. Nauk SSSR, Mekh. Zhidk. Gaza*, No. 5, 78–85 (1989).
6. M. V. Filinov, V. M. Maksimov, and A. M. Ber, "Mathematical model of joint filtration of mutually soluble liquids," in: *Trans. of the Moscow Institute of Oil and Gas Industry* [in Russian], No. 186, Moscow (1986).
7. G. F. Trebin, Yu. F. Kapyrin, and O. G. Limanskii, *Estimate of Temperature Depression in the Bottom-Hole Zone of Production Wells* [in Russian], No. 64, Gas and Oil Inst., Moscow (1978), pp. 16–22.
8. I. L. Khabibullin and R. F. Sharafutdinov, "Estimate of heat of gas solution in liquids," in: *Collection of Scientific Papers* [in Russian], Izd. Bashkir. Univ., Ufa (1995), pp. 144–146.